BIOCHEMICAL PHARMACOLOGY 76 (2008) 1503–1514

available at www.sciencedirect.com

ScienceDirect

journal homepage: www.elsevier.com/locate/biochempharm

Pleiotropic effects of selective CDK inhibitors on human normal and cancer cells

Józefa Węsierska-Gądek [a,*], *Susanne B. Hajek* [a], *Bettina Sarg* [b], *Stefanie Wandl* [a], *Eva Walzi* [a], *Herbert Lindner* [b]

[a] *Cell Cycle Regulation Group, Department of Medicine I, Div.: Institute of Cancer Research, Medical University of Vienna, Vienna, Austria*
[b] *Division of Clinical Biochemistry, Biocenter, Medical University of Innsbruck, Innsbruck, Austria*

ARTICLE INFO

Article history:
Received 1 June 2008
Accepted 15 July 2008

Keywords:
CDK inhibitors
Cell cycle arrest
HPV18
p53 Tumor suppressor
E6 oncoprotein
CLIMP-63

ABSTRACT

Escape from the proper control of the cell cycle by up-regulation of cyclins or aberrant activation of cyclin-dependent kinases (CDKs) as well as by inactivation of cellular inhibitors of CDKs (CKI) leads to malignant transformation. Loss of cellular CKIs in cancers provided a rationale for development of pharmacological inhibitors of CDKs. Recently synthesized CKIs, e.g., purine derivatives such as olomoucine (OLO) and roscovitine (ROSC) are non-genotoxic and exhibit increased selectivity towards CDK2 and CDK7/9. Interestingly, both drugs induce additional effects. Recently, a new, unexpected action of OLO on normal human cells was observed. OLO strongly up-regulates CLIMP-63, a 65 kD protein that mediates the anchoring of the ER to microtubules. Moreover, ROSC induces in human MCF-7 cells phosphorylation of p53 protein at Ser-46 which in turn initiates caspase-independent apoptosis.

In the present contribution we raised the question whether both CKIs would be able to block cell cycle progression and to reactivate p53 protein in human HPV-positive HeLa cervix carcinoma cells. We also addressed the question whether exponentially growing cancer cells are more susceptible to the inhibitory action of CKIs than normal cells. Our results show that HeLa cells are much more sensitive to ROSC than normal fibroblasts. ROSC induces G_2 arrest and apoptosis in HeLa cells. It also reactivates and stabilizes wt p53 protein. The increase of p53 protein coincides with down-regulation of E6 oncoprotein.

Thus, the biological action of substituted purines is not restricted to the inhibition of CDKs and open new perspectives for their therapeutic applications.

1. Introduction

The progression of the mammalian cell cycle is driven by transient activation of complexes consisting of cyclins and cyclin-dependent kinases (CDKs) [for reviews, see Refs. [1–3]]. The escape from the proper control of the cell cycle by up-regulation of cyclins, by constitutive activation of CDKs as well as by inactivation of cellular inhibitors of CDKs (CKI) or tumor

* *Corresponding author at*: Department of Medicine I, Div.: Institute of Cancer Research, Cell Cycle Regulation Group, Vienna Medical University, Borschkegasse 8 a, A-1090 Vienna, Austria. Tel.: +43 1 4277 65247; fax: +43 1 4277 65194.
E-mail address: Jozefa.Gadek-Wesierski@meduniwien.ac.at (J. Węsierska-Gądek).

Abbreviations: CDK, cyclin-dependent kinase; CKI, cyclin-dependent kinase inhibitor; CKAP4/p63, cytoskeleton-associated protein 4/p63; CLIMP-63, cytoskeleton-linking membrane protein-63; ER, endoplasmic reticulum; FACS, fluorescence-activated cell sorting; HIPK2, homeodomain protein kinase2; OLO, olomoucine; PDL, population doubling level; PI, propidium iodide; PVDF, polyvinylidene difluoride; ROSC, roscovitine; WCL, whole cell lysate; MS/MS, tandem mass spectrometry.

0006-2952/$ – see front matter
doi:10.1016/j.bcp.2008.07.040

suppressor proteins such as pRb and p53 leads to development of cancer [for reviews, see Refs. [4–8]]. For these reasons the activated cyclin–CDK complexes have been considered as very promising therapeutic targets in human malignancies [9]. Moreover, loss of cellular CKIs in cancers provided a rationale for development of pharmacological inhibitors negatively affecting the activity of CDKs. Furthermore, it has also been recognized that the (re)activation of the endogenous wt p53 in cancer cells may substantially contribute to the positive outcome of chemotherapy [10,11]. In the mid 90s first pharmacological inhibitors of CDKs were generated by a Czech group [12]. They had a relatively low specificity and inhibited a broad range of cellular kinases. Later, more selective compounds were synthesized [13–15]. Currently available pharmacological CDK inhibitors represent a few distinct classes of compounds and exert different target specificity [16,17]. Some of them, e.g., flavopiridol and roscovitine (ROSC) have been found to markedly increase levels of p53 tumor protein suppressor protein [18,19]. Considering the fact that rapidly dividing cancer cells and normal, healthy cells differ in the pattern of the expression of cell cycle regulators, in CDK activities, and in the p53 status, one might expect that anti-proliferative efficiency of the pharmacological CDK inhibitors would depend on the mitotic index of treated cells.

Pharmacological inhibitors of CDKs belonging to purine derivatives such as ROSC and olomoucine (OLO) are non-genotoxic and exhibit increased selectivity towards CDK2 and CDK7/9 [13–15]. Interestingly, both drugs exert additional effects [20–22]. We studied recently the effects of ROSC and OLO on asynchronously growing human MCF-7 breast cancer cells that express wt p53 protein. In these cells effector caspase-3 is inactivated due to a deletion of a 47-bp fragment within exon 3 of the *caspase-3* gene [23]. As a consequence MCF-7 cells are resistant to the action of a variety of conventional cytostatic drugs [24,25]. We observed that ROSC inhibited proliferation and induced a strong cell cycle arrest of the human asynchronously growing MCF-7 breast cancer cells beginning at 6 h after onset of the treatment [21,26]. Inhibition of DNA replication and accumulation of G_2/M arrested cells coincided with a marked up-regulation of p53 protein and with the appearance of a few Annexin-V positive cells and preceded the main wave of apoptosis occurring after exposure of MCF-7 cells to ROSC for 24 h [21]. Moreover, ROSC resulted in the nuclear accumulation of p53 protein and its significant stabilization [21,26]. Interestingly, ROSC-induced site-specific phosphorylation of p53 protein [26]. Unlike other agents, ROSC did not induce phosphorylation of p53 protein at Ser-15 and Ser-20 [22,26], but modified p53 at the serine residue at position 46 [26]. The onset of phosphorylation of Ser-46 preceded the appearance of p53AIP1 protein [26], a specific downstream target of site-specifically phosphorylated p53 transcription factor [27]. p53AIP1 protein, induced by the p53 isoform phosphorylated at Ser-46, accumulated after *de novo* synthesis in the cytosol and then moved into the mitochondria [26]. Analyses of the enzymatic activity revealed that homeodomain-interacting protein kinase-2 (HIPK2) but not ATM kinase was activated by ROSC in MCF-7 cells [28]. The overexpression of wt but not mutant HIPK2 increased the basal and ROSC-induced level of p53 phosphorylation at Ser-46 and strongly enhanced the rate of apoptosis in cells exposed to ROSC [28]. These observations raised the question whether ROSC would also be efficient in the treatment of cancers with viral etiology, e.g., HPV-positive cervix carcinoma. Considering the fact that cellular CDKs are required for nuclear viral DNA replication and transcription, pharmacological inhibitors of CDKs also possess anti-viral activities [29,30].

Therefore, in the present paper we examined the susceptibility of virally transformed human cancer cells to two related purine-based inhibitors namely OLO and ROSC, and compared with that of normal human fibroblasts. Unlike ROSC, OLO is a much weaker inhibitor of CDKs. Both inhibitors inhibited proliferation of human HeLa cervix carcinoma cells. However, much higher concentration of OLO was necessary to reduce the number of living cells by 50%. Exposure of HeLa cells to ROSC resulted in a marked increase of cellular p53 protein levels due to its stabilization that coincided with a decrease of the level of E6 oncoprotein. As expected, both CDK inhibitors showed a weak anti-proliferative effect on non-transformed human fibroblasts. Surprisingly, their exposure to OLO but not to ROSC resulted in an induction of a protein with 65 kD in a dose- and time-dependent manner. Mass spectrometric analysis of the Coomassie-blue-stained up-regulated protein revealed that the cytoskeleton-linking membrane protein-63 (CLIMP-63) [20] is a major component of the strong protein band. The identity of this protein was confirmed by immunoblotting experiments. These results clearly demonstrate that even less potent pharmacological CDK inhibitors exert strong biological effects on normal tissues.

Thus, CDK inhibitors exert pleiotropic effects on normal and cancer cells and they interact with cell specific targets.

2. Material and methods

2.1. Cell culture

Normal human MRC-5 skin and F2000 lung fibroblasts, as well as human HeLa cervix carcinoma cells were used in this study. MRC-5 and F2000 cells were grown up to 60–70% confluence as a monolayer in Dulbecco's medium supplemented with 10% fetal calf serum in an atmosphere of 8% CO_2. HeLa cells were grown as suspension culture in RPMI medium with 10% fetal calf serum in an atmosphere of 5% CO_2. Cells were treated with ROSC and OLO at a final concentration ranging from 1 to 150 μM for indicated periods of time.

2.2. Antibodies

We used the following antibodies: monoclonal anti-CLIMP-63 (G1/296) (Alexis Biochemicals, San Diego, CA) and polyclonal antibody (a kind gift from Dr. J. Rohrer) [31], monoclonal anti-PCNA (clone PC-10) antibody (Oncogene Research Products, Cambridge, MA), monoclonal anti-MCM-7 (clone DCS141.2) antibody and anti-Rb antibody (IF-8) (Santa Cruz Biotechnology, Inc., Santa Cruz, CA), p53 DO-1 antibody which was a kind gift from Dr. B. Vojtesek (Masaryk Memorial Cancer Institute, Brno), and monoclonal anti-actin antibody (Clone C4) from ICN Biochemicals (Aurora, OH, USA). Polyclonal antibodies recognizing site-specific phosphorylation of CDKs and of Rb protein

as well as total CDKs were from New England Biolabs (Beverly, MA). Fluorescein-conjugated monoclonal mouse antibodies M30 CytoDEATH, recognizing only caspase-3 cleaved cytokeratin 18, were from Roche Applied Science (Penzberg, Germany).

2.3. Determination of the number of viable cells

Proliferation of human cells and their sensitivity to increasing concentrations of drugs were determined by the CellTiter-Glo® Luminescent Cell Viability Assay (Promega Corporation, Madison, WI). As described recently in more detail [32], the CellTiter-Glo® Luminescent Cell Viability Assay, generating luminescent signals, is based on quantification of the cellular ATP levels. Tests were performed at least in quadruplicates. Luminescence was measured in the Wallac 1420 Victor, a multilabel, multitask plate counter. Each point represents the mean ± S.D. (bars) of replicates from at least three experiments.

2.4. Measurement of the caspase-3 activity

Activity of the caspases 3/7 was determined in multiwell plates using the homogeneous, luminescent Caspase-Glo™ 3/7 assay (Promega Corp., Madison, WI) as described previously in more detail [33,34]. The Caspase-Glo™ 3/7 assay provides a proluminescent caspase-3/7 substrate, which contains the tetrapeptide sequence DEVD that is recognized by both effector caspases. The addition of a single Caspase-Glo™ 3/7 reagent in an ''add-mix-measure'' format results in cell lysis, followed by caspase-mediated cleavage of the DEVD motif. This releases a substrate for luciferase (aminoluciferin) that generates a ''glow-type'' luminescent signal. Luminescence is proportional to the amount of caspase activity present in the samples. Fresh medium (no cells = no caspase) was used as a blank. The measured values (relative luminescence units, RLU) were blank subtracted and normalized against the number of viable cells present in the wells. The latter were parallelly determined using CellTiterLumiGlo. Each point represents the average of four replicates.

2.5. Measurement of DNA content in single cells by flow cytometry

The measurement of DNA content was performed by flow cytometric analysis based on a slightly modified method [35] described previously by Vindelov et al. [36]. Propidium iodide (PI)-stained cells were measured by flow cytometry using the Becton Dickinson fluorescence-activated cell sorter (FACScan). Distribution of cells in distinct cell cycle phases was determined using ModFIT cell cycle analysis software. DNA histograms were obtained by the CellQuest evaluation program.

2.6. Detection of apoptotic cells by CytoDEATH staining

Apoptotic cells were detected by M30 CytoDEATH monoclonal antibodies (Roche Molecular Biochemicals, Vienna, Austria) recognizing caspase-3 cleaved cytokeratin 18. Apoptotic cells were detected *in situ* by indirect immunofluorescence microscopy and were additionally quantified by flow cytometric analysis [34]. For microscopic analysis cells were plated on slides in plastic chambers and appropriately cultivated. After treatment for indicated time, cells were washed three times in PBS, fixed and stained with the fluorescein-coupled M30 CytoDEATH monoclonal antibodies according to the manufacturer's protocol. M30 CytoDEATH stained cells were quantified by flow cytometric and inspected under a fluorescence microscope (inverted microscope Eclipse TE300, Nikon Corporation, Tokyo) [33,34].

2.7. Quantitative analysis of the mitochondrial membrane potential by flow cytometry

Depolarization of mitochondrial membrane was monitored using the cationic carbocyanine dye JC-1 (Molecular Probes Inc., Eugene, OR, USA) as previously described [26].

2.8. Mass spectrometric analysis

Unless otherwise noted, the various steps of the procedure were performed at room temperature and all incubation steps were performed under shaking. The protein band of interest in the SDS-gel was excised, cut into small pieces, transferred into a 0.25-ml polyethylene sample vial and washed twice with 150 μl, 10 mM NH_4HCO_3, pH 8.9 (15 min at 30 °C). The supernatant was discarded and the gel pieces were shrunk by dehydration in 150 μl of 50% (v/v) acetonitrile/10 mM NH_4HCO_3 (15 min at 30 °C). This step was performed twice and, after removing all liquid, the gel pieces were dried in a vacuum centrifuge. The gel pieces were swollen in a digestion buffer containing 10 mM NH_4HCO_3 and 0.05 μg/μl of trypsin (Roche, sequencing grade) at 4 °C for 20 min. The supernatant was removed and replaced with 20 μl of the same buffer without trypsin. Digestion took place overnight at 37 °C. Peptides were extracted by adding 50 μl, 10 mM NH_4HCO_3 (37 °C, 15 min), and 50 μl acetonitrile (37 °C, 15 min). After collecting the supernatant 100 μl, 10% formic acid/20% acetonitrile/20% 2-propanol was added to the gel pieces (37 °C, 10 min). The supernatants were combined, concentrated by drying to approximately 5 μl, and stored at –20 °C. Tryptic protein digestions were analysed using capillary HPLC connected on-line to an LCQ ion trap instrument (ThermoFinnigan, San Jose, CA, USA) equipped with a nanospray interface. The nanospray voltage was set at 1.6 kV and the heated capillary was held at 170 °C. MS/MS spectra were searched against a human protein database using SEQUEST (LCQ BioWorks; ThermoFinnigan).

2.9. Electrophoretic separation of proteins and immunoblotting

Total cellular proteins dissolved in SDS sample buffer were separated on 10% SDS slab gels and transferred electrophoretically onto polyvinylidene difluoride (PVDF) membranes (Amersham International, Little Chalfont, Buckinghamshire, England). Equal protein loading and protein transfer was confirmed by Ponceau S staining. Blots were incubated with specific primary antibodies at the appropriate final dilution and the immune complexes were detected using appropriate

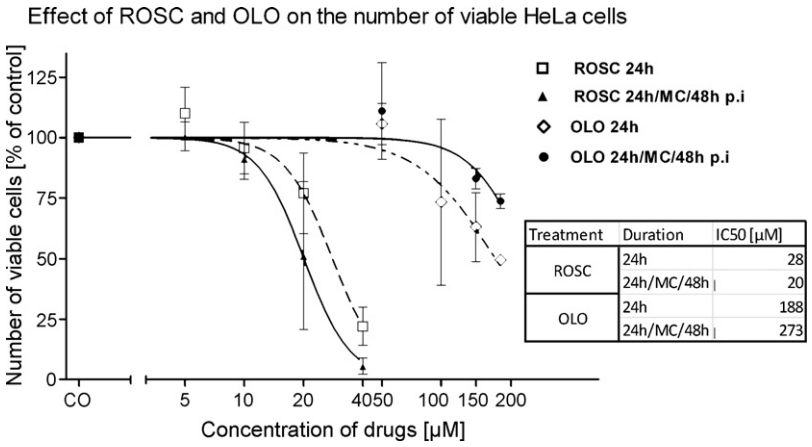

Fig. 1 – ROSC stronger reduces the number of viable human HeLa cervical cancer cells than OLO. Exponentially growing HeLa cells plated in 96-well microtiter plates were treated for 24 h with increasing concentrations of ROSC and OLO. The number of viable cells was determined directly after treatment (24 h) and additionally, after post-incubation for 48 h in a drug-free medium (24 h/MC/48 h). The graph represents mean values ± S.D. from three independent experiments, each performed at least in quadruplicates. IC_{50} values for both drugs are indicated.

peroxidase-conjugated secondary antibodies and the enhanced chemiluminescent detection reagent ECL+ (Amersham International, Little Chalfont, Buckinghamshire, England). In some cases, blots were used for several sequential incubations. Incubation with anti-actin antibodies additionally confirmed equal protein loading [32,33].

2.10. *Statistical analysis*

Statistical analyses were performed using GraphPad Prism and significance levels were evaluated using Dunnett's Multiple Comparison test.

3. Results

3.1. *ROSC stronger inhibits proliferation of exponentially growing HeLa than OLO*

In agreement with our previous observations [37], treatment of HeLa cells for 24 h with increasing ROSC concentrations resulted in a clear reduction of the number of viable cells in a concentration-dependent manner (Fig. 1). At a final concentration of 28.2 μM the number of viable cells was reduced by 50%. We also checked whether the inhibitory effect of ROSC is transient or may persist in the absence of the drug. For this purpose we treated cells with ROSC for 24 h and then after medium change cells were post-incubated in a drug-free medium for the further 48 h. As depicted in Fig. 1, after post-incubation the number of viable cells decreased. IC_{50} was reduced by approximately 30% thereby evidencing that the inhibition of CDKs in HeLa cells has long-term effects. Unlike ROSC, OLO exerts a much weaker anti-proliferative effect. An approximately seven-fold higher dose of OLO was necessary to reduce the number of living HeLa cells by 50% (Fig. 1). Moreover, the inhibitory effect of OLO was transient. After post-incubation of OLO-treated HeLa cell for 48 h in a drug-free medium the number of HeLa cells slightly increased (IC_{50} = 273 μM). This indicates that OLO-treated HeLa cells very rapidly re-entered the active cell cycle.

3.2. *Normal fibroblasts are less susceptible to the action of pharmacological inhibitors of CDKs*

It has been previously evidenced that ROSC and OLO affected human MRC-5 cells only at high doses [20]. In the present paper we examined additionally F2000 cells, normal human fibroblasts. Treatment of human F2000 cells for 24 h with both inhibitors slightly diminished their number (Fig. 2). However, after post-incubation of OLO-treated F2000 cells for 48 h in a drug-free medium the number of viable cells was markedly diminished (Fig. 2). The difference between controls and cells treated with 150 μM OLO was statistically very significant ($p < 0.01$). Similar effects were observed after exposure of MRC-5 cells to CKIs (not shown).

3.3. *ROSC increases ratio of G_2 arrested HeLa cells and after longer time induces apoptosis*

Determination of the DNA concentration in PI stained cells revealed that ROSC primarily inhibits the cell cycle progression of HeLa cells (Fig. 3A), and at higher concentrations induces apoptosis (Fig. 3B), but has a low effect, if any, on the distribution of MRC-5 (Fig. 4) and F2000 cells (not shown) in cell cycle phases. After exposure of HeLa cells to ROSC at higher concentrations for 24 h an accumulation of the G_2/M cell population became evident (Fig. 3B). At a final concentration of 40 μM ROSC the ratio of hypoploid cells representing cells undergoing apoptosis increased (Fig. 3B). The accumulation of G_2/M cells coincided with the increase of the inhibitory phosphorylation of CDK1 (at Thr14/Tyr15) (not shown) thereby indicating that ROSC arrested cells in the G_2 phase of the cell cycle. Unlike ROSC, OLO affected HeLa cells much weaker. No accumulation of hypoploid cells and a slight

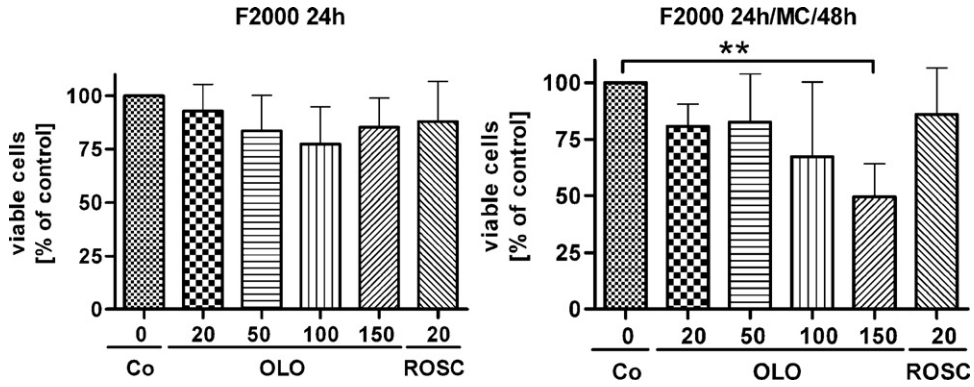

Fig. 2 – Long-term effect of OLO on the proliferation of human F2000 fibroblasts. Dividing human F2000 fibroblasts plated in 96-well microtiter plates were treated for 24 h with increasing concentrations of OLO and ROSC. The number of viable cells was determined directly after treatment (24 h) and additionally, after post-incubation for 48 h in a drug-free medium (24 h/MC/48 h). The graph represents mean values ± S.D. from three independent experiments, each performed at least in quadruplicates. IC_{50} = 182 μM OLO after treatment for 24 h, medium change and post-incubation for 48 h. Statistical analyses were performed using GraphPad Prism and significance levels were evaluated using Dunnett's Multiple Comparison test. The reduction of the number of viable cells after exposure to 150 μM OLO for 24 h/MC/48 h was very significant ($p < 0.01$).

increase of G_2/M cells were observed 24 h after onset of treatment (Fig. 3C).

The distribution of human MRC-5 cells in distinct cell cycle phases was not changed after their exposure for 24 h to both CKIs (Fig. 4). These observations are in concordance with the results of cell proliferation assay (Fig. 2).

3.4. ROSC increases the concentration of p53 protein in HeLa and in MRC-5 cells

Analysis of cell lysates by immunoblotting revealed that cellular levels of p53 protein markedly increased in human HeLa cells (Fig. 5) and MRC-5 cells (Fig. 6) exposed to ROSC. Interestingly, OLO has much weaker effect on the cellular level of p53 protein. OLO has no effect on p53 levels in HeLa cells (Fig. 5) but resulted in a weak increase of p53 protein in MRC-5 cells (Fig. 6A). Unlike in HeLa cells, in human MRC-5 fibroblasts the basal p53 expression is higher and even in untreated control cells p53 protein is detectable (Fig. 6A and B). Remarkably, ROSC is able to elevate the p53 concentration not only in cycling but also in quiescent MRC-5 cells (Fig. 6). The latter are characterized by a down-regulation of MCM-7 protein (Fig. 6B).

3.5. ROSC stabilizes p53 protein in HeLa cells

p53 protein is generally a short-lived protein and in HeLa cells its half-life is additionally shortened by the inactivating interaction with HPV-encoded E6 oncoprotein. Therefore, the question appeared whether ROSC would be able to prevent the accelerated p53 degradation. For this purpose the stability of p53 protein was examined in control cells and cells exposed to ROSC for 15 h. To determine the half-life of proteins, their synthesis was blocked by addition of emetine to cell culture and then after post-incubation for different periods of time cells were lysed. WCLs from control and ROSC-treated cells were loaded on the same slab gel, and after electrotransfer onto PVDF membrane p53 protein was detected by immunoblotting. As shown in Fig. 7A, in control cells p53 signal was very weak. In contrast, the intensity of p53 protein band was very strong in ROSC-treated samples and it only slightly decreased after post-incubation for 60 min (Fig. 7A). This clearly evidences that ROSC markedly increased the stability of p53 protein. This observation evoked the question how does it work? Is ROSC able to prevent p53 targeting by E6-AP ubiquitin ligase recruited by E6 oncoprotein or does ROSC inhibit the transcription of the virally encoded E6 protein. Our preliminary results (Fig. 7B) indicate that ROSC repressed the E6 protein. After 12 h ROSC the intensity of E6 protein band was clearly diminished.

3.6. Reduced activity status of CDKs in cells exposed to ROSC

To evaluate the real effect of ROSC on the activity status of CDKs, we examined its action on the site-specific phosphorylation of CDK2 and CDK7. As depicted in Fig. 7C and D, after administration of ROSC at a final concentration of 40 μM the activating phosphorylation of CDK2 at Thr160 and of CDK7 at Ser167/Thr170 was abolished. The lack of the activating phosphorylation of CDK2 correlated with the appearance of Rb protein that was unphosphorylated at Ser780 (Fig. 7D). Interestingly, the prevention of the phosphorylation of CDK7 has implications not only for the cell cycle progression but also for transcription of both cellular and virally encoded genes and elucidates the mechanism of the ROSC-mediated repression of E6 oncoprotein.

3.7. ROSC induces caspase-dependent apoptosis

Accumulation of sub-G_1 cells after ROSC treatment focused our attention on the pathway of programmed cell death. Inspection of the reactivity pattern of anti-PARP-1 antibodies on immunoblots (Fig. 5) revealed an appearance of an 89 kD

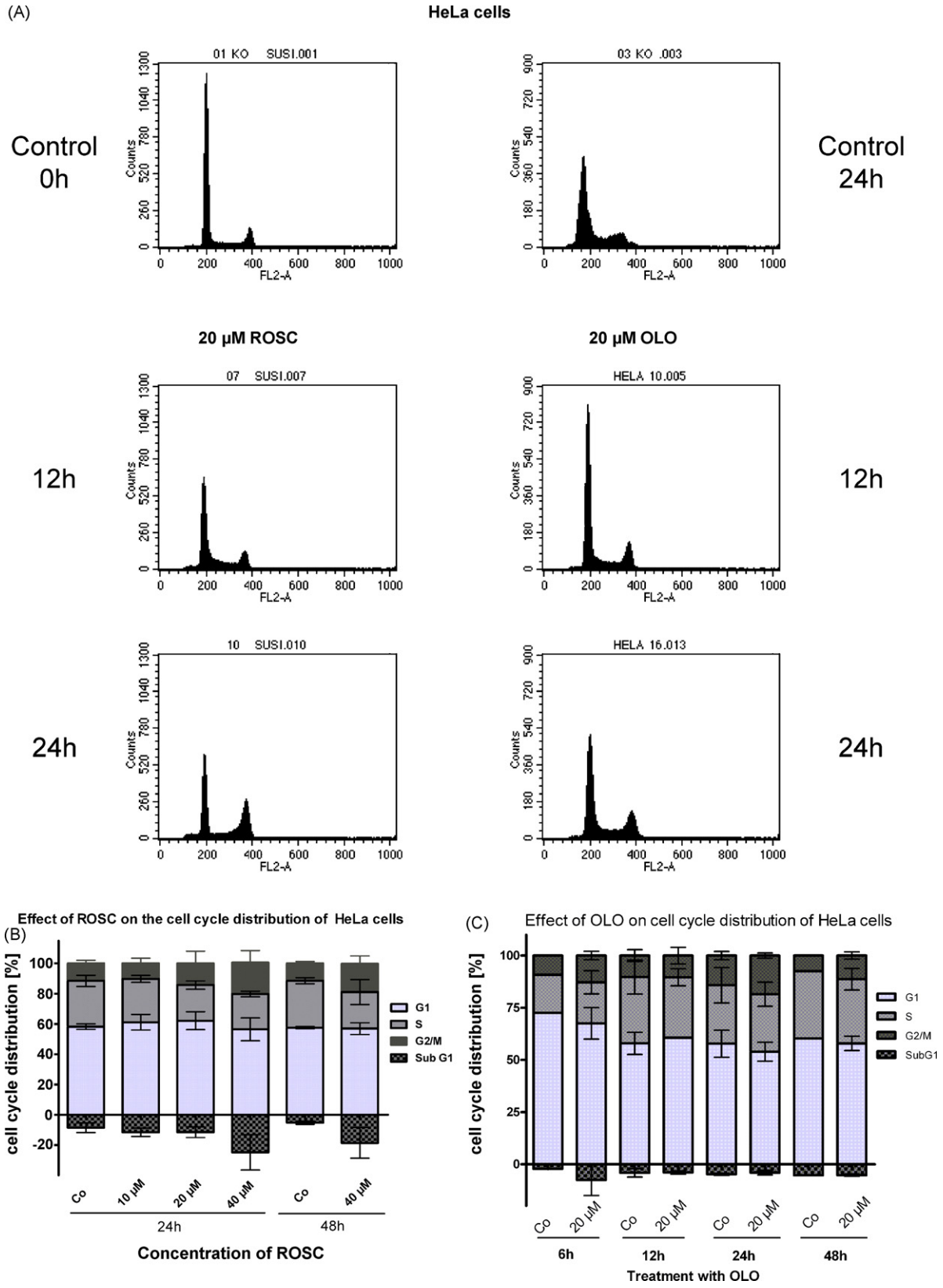

Fig. 3 – ROSC but not OLO induces cell cycle arrest and apoptosis in HeLa cells. The cells were treated with 20 μM ROSC or 20 μM OLO for the indicated periods of time. (A) Example FACS profiles of propidium iodide-stained control cells, and cells treated with ROSC or OLO, respectively. (B) Effect of ROSC on the distribution of HeLa cells in distinct cell cycle phases. HeLa cells were continuously exposed to ROSC at indicated concentrations for 24 h or 48 h. The graph represents mean values ± S.D. from three independent experiments. ROSC at higher concentrations blocks HeLa cells in G_2 phase of the cell cycle and induces apoptosis. Continuous treatment with 40 μM ROSC for 48 h did not increase apoptotic rate. (C) Effect of

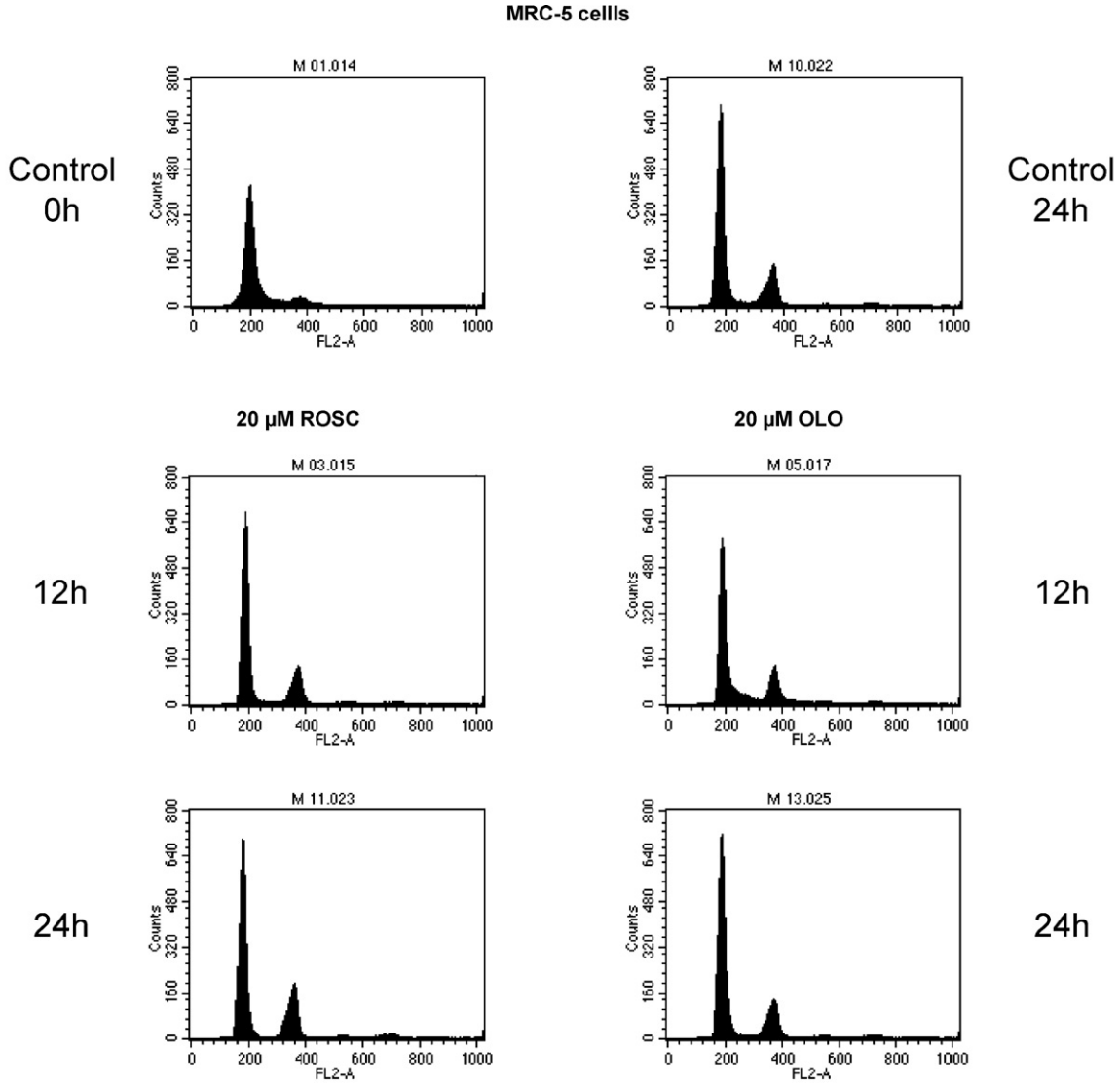

Fig. 4 – ROSC and OLO do not affect the progression of cell cycle in human MRC-5 cells. MRC-5 cells were treated with 20 μM ROSC or 20 μM OLO for the indicated periods of time. DNA histograms of propidium iodide-stained control cells, and cells treated with ROSC or OLO, respectively are shown.

band corresponding to the caspase-3 cleaved fragment of PARP-1 in samples obtained from CKI-treated cells. The monitoring of the activity status of caspase-9 (Fig. 5) shows the appearance of a cleaved form of caspase-9 (p18) in cells exposed to ROSC. After ROSC treatment for 24 h the intensity of procaspase-9 strongly decreased. This correlates with the major peak of the hypoplopid cells. Therefore, to unambiguously prove the pro-apoptotic effect of ROSC on HeLa cells, we performed a few experiments to find out whether ROSC treatment has any effect on the potential of the mitochondrial membrane and on the activity of effector caspases, e.g., caspase-3 and -7. The cytometric bivariate analysis of the aggregation status of the cationic dye JC-1 revealed that approximately 20% of HeLa cells lost the ability to aggregate the dye upon treatment of cells with ROSC for 24 h (Fig. 8A). It became evident that a higher dose of ROSC is necessary to reduce the potential of the mitochondrial membrane (Fig. 8A). Moreover, the activation of effector caspases in ROSC-treated HeLa cells was evidenced by another test. Using for immunofluorescence staining and flow cytometry specific antibodies reacting solely with caspase-3 cleaved targets, strong signals for cleaved PARP-1 (not shown) and cytokeratine 18 (M30 CytoDEATH, Fig. 8B) positive cells appeared after treatment with ROSC. As depicted in Fig. 8B, in untreated controls approximately 3% cells were stained and after exposure for 12 h to 40 μM ROSC the ratio of M30 CytoDEATH-stained cells increased by 10%. We also determined the activity of caspase-3/7 in HeLa cells exposed to ROSC. An eight-fold increase of the

OLO on the distribution of HeLa cells in distinct cell cycle phases. The graph represents mean values ± S.D. from three independent experiments. HeLa cells were continuously exposed to 20 μM OLO for indicated periods of time.

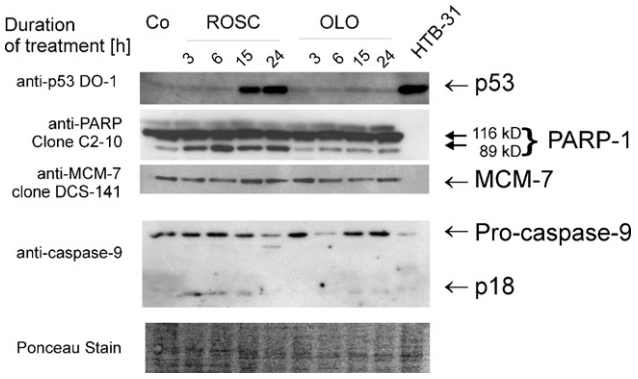

Fig. 5 – ROSC but not OLO reactivates p53 protein in HeLa cells. Whole cell lysates (WCLs) were prepared from control cells and cells exposed to 20 μM ROSC or to 20 μM OLO for indicated periods of time. Proteins (30 μg protein/well) were separated on 10% or 12% SDS polyacrylamide gels and transferred onto PVDF membrane. WCL prepared from human HTB31 cervix carcinoma cells, that express mutated p53 protein, was loaded as a p53 positive control. Blots were incubated with primary antibodies as indicated. Proper transfer of proteins and equal protein loading was checked by Ponceau S staining. Immune complexes were labelled with appropriate secondary antibodies coupled to HRP and finally detected using ECL+ as a substrate.

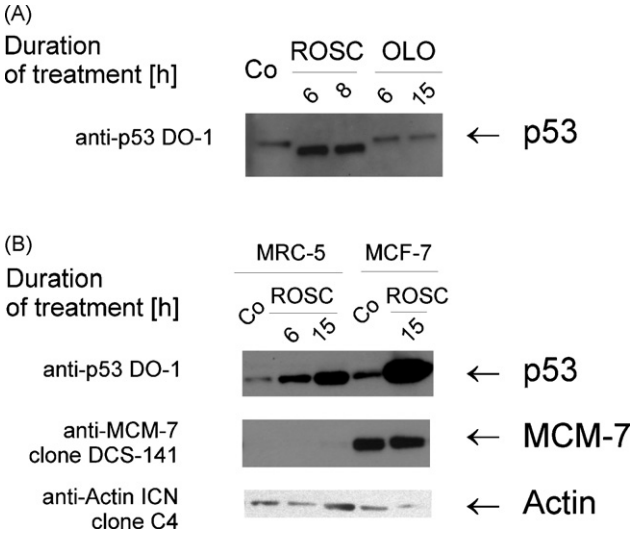

Fig. 6 – Effect of ROSC and OLO on cellular levels of p53 protein in MRC-5 cells. Whole cell lysates (WCLs) were prepared from control cells and cells exposed to 20 μM ROSC or to 20 μM OLO for indicated periods of time. Proteins (30 μg protein/well) were resolved on 10% SDS polyacrylamide gels and transferred onto PVDF membrane. Blots were incubated with primary antibodies as indicated. Conditions of immunoblotting as described in detail in Fig. 5.

caspase-3/7 activity was observed after treatment with 40 μM ROSC for 18 h (Fig. 8C).

3.8. *Increase of CLIMP-63 protein in OLO-treated human MRC-5 fibroblasts*

Human MRC-5 cells were exposed to both CKIs at a final concentration of 20 μM. In concordance with our previous report, OLO but not ROSC elevated the intensity of a protein band at 65 kD (Fig. 9A). Using mass spectrometry for analysis of the excised bands the CLIMP-63 protein was identified as its major component. The identity of the protein was further confirmed by immunoblotting (Fig. 9B). As shown in Fig. 9A, in control MRC-5 cells and cells treated with ROSC signals for CLIMP-63 protein were not detectable. In contrast, in cells exposed to OLO for 24 h CLIMP-63 a strong signal appeared. These results confirm our previous. However, the analysis of the time course of the accumulation of CLIMP-63 protein of the protein revealed that it is induced with varying kinetics.

4. Discussion

The human genome encodes for 13 putative CDKs [38]. Based on their functions, CDKs can be classified in two major groups: those involved in the control of the cell cycle and others responsible for transcriptional regulation. Cell cycle regulatory CDKs 1, 2, 3, 4, and 6 associate with corresponding cyclins drive the cell cycle progression and cell division. Transcriptional kinases like CDK8 with cyclin C and CDK9 with cyclin T (pTEFb), constitute a second non-overlapping group of the CDKs. They promote initiation and elongation of nascent RNA transcripts by phosphorylation of the largest subunit of RNA polymerase II [39–42]. One CDK, namely CDK7 complexed with cyclin H, also implicated in the regulation of transcription, cannot be simply classified. It provides a direct link between regulation of cell cycle and transcription, because it is both, a CDK-activating kinase (CAK) and a constituent of the basal transcription factor TFIIF, which phosphorylates the serine residues within the heptapeptide repeat of the carboxy terminal domain (CTD) of RNA polymerase II [39].

The selective, pharmacological CDK inhibitors (from the purine family) compete with ATP and can be pan-specific and oligo- or mono-specific. ROSC and OLO are oligo-specific and preferentially inhibit only a subset of CDKs. Interestingly, ROSC is non-toxic and in pre-clinical and in clinical trials its high efficacy was so far attested [17]. Currently, ROSC is in phase II clinical trials for breast cancer, small cell lung carcinoma and glomerulonephritis [17]. Interestingly, pharmacological inhibitors of CDKs exert additional, very promising activities. Since a number of viruses require cellular CDKs for their DNA synthesis, the inhibition of CDKs might prevent their replication and thereby would display anti-viral effects [29]. Indeed, several purine-based CKIs including ROSC have anti-viral activity [30]. It has been shown that ROSC blocks replication of HIV, HCMV, EBV as well as of HSV-1 and -2 [30]. However, the exact mechanisms by which the CKIs prevent the replication of the anti-viral but not cellular genome is still not clear. Therefore, the anti-viral mechanisms and targets of CKIs have to be carefully investigated and characterized.

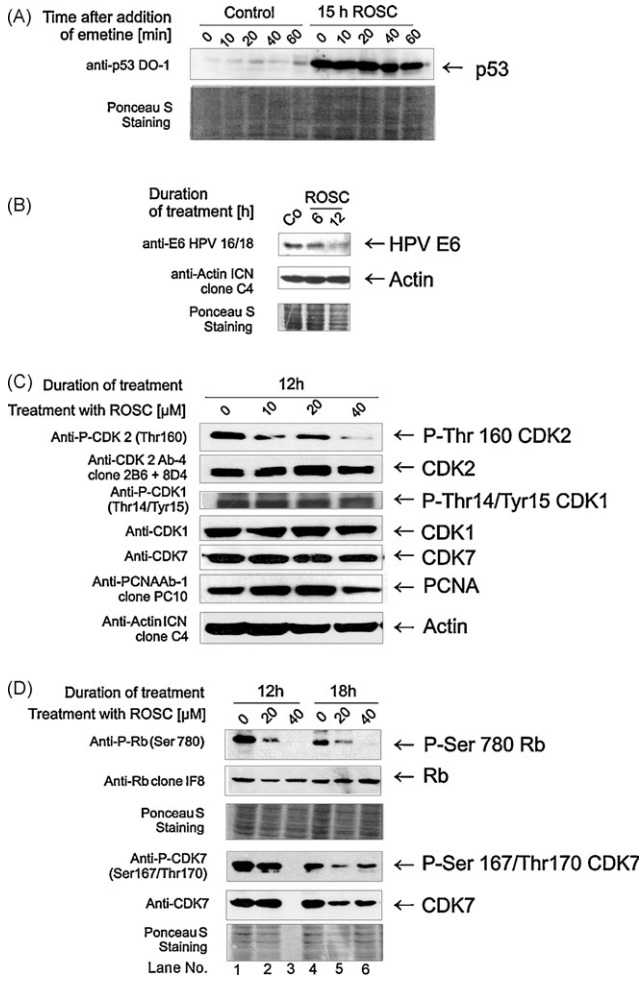

Fig. 7 – ROSC stabilizes p53 protein in HeLa cells by repression of E6 oncoprotein. (A) ROSC increases the half-life of p53 protein in HeLa cells. Control cells and cells exposed for 15 h to 20 μM ROSC were treated with emetine, an inhibitor of protein synthesis. WCLs were prepared immediately after addition of emetine and at different time points after post-incubation as indicated. Proteins were resolved on 10% SDS polyacrylamide gels and transferred onto PVDF membrane. Blots were incubated with antibodies as indicated. Proper transfer of proteins and equal protein loading was checked by Ponceau S staining. (B) Decrease of the levels of E6 protein after exposure of HeLa cells to ROSC. WCLs were separated on 15% SDS polyacrylamide slab gels. Blots were incubated with antibodies as indicated. (C) ROSC abolishes the activating phosphorylation of CDK2. WCLs prepared from untreated controls (0 h) and cells exposed to ROSC at indicated concentrations for 12 h were separated on 12% SDS polyacrylamide slab gels. Blots were incubated with antibodies as indicated. (D) ROSC inhibits site-specific phosphorylation of CDK7 determining its transcriptional activity. WCLs prepared from untreated controls (0) and cells exposed to ROSC at indicated concentrations for 12 h and 18 h were separated on 12% SDS polyacrylamide slab gels. In the third lane of the lower gel a molecular weight marker was loaded instead of WCL sample.

In this contribution we examined the action of two purine-based CKIs: ROSC and OLO on the proliferation and cell cycle progression of HeLa cells. Human HeLa cervical carcinoma cells express E6 and E7 oncoproteins, products of the high-risk HPV18. These small proteins exert profound effects on the tumor suppressor proteins pRb and p53. E7 binds to pRb resulting in destabilization and finally disruption of Rb/E2F repressor complexes. E6 oncoprotein recruits cellular E6-AP and targets p53 for ubiquitylation and enhanced proteasome-mediated degradation [43,44]. These interactions disrupt the restriction checkpoint between G_1 and S phase. As a consequence HPV-positive cells escape from the proper cell cycle control and may acquire additional mutations driving tumor progression. It has been recognized that repression of HPV-encoded oncoproteins reactivates p53 and pRb proteins and restores tumor suppressor pathways. Different strategies were developed to eradicate both HPV-encoded oncoproteins from HeLa cells [45,46]. Considering the anti-viral properties of ROSC, one would expect that it would be able to restore normal function of p53 and pRb. Our results show that ROSC blocks cell cycle progression and reactivates p53 in HeLa cells. It coincides with the repression of E6 protein. How to explain the diminution of the cellular levels of E6 protein upon ROSC treatment? As evidenced in this publication, ROSC abolished the activating phosphorylation of CDK2 and CDK7. The reduction of the site-specific phosphorylation at the T-loop of CDK2 detected already after exposure to ROSC for 12 h correlated with the decrease of the phosphorylation of Rb protein. The prevention of phosphorylation of CDK7 is a convincing proof of the effectiveness of ROSC treatment. CDK7 is at the crossroad between two processes: cell cycle and transcription. The direct connection between regulation of the activity status of CDKs and transcription machinery maintained by CDK7 implicates that it accepts two distinct substrates. It is not clear how these two functions might be timely and spatially coordinated. The question how CDK7 is able to discriminate between two targets is partially elucidated. It has been suggested that phosphorylation of Thr170 greatly stimulates the activity of the CDK7/cyclin H/MAT1 complex towards the C-terminal domain of RNA polymerase II without significantly affecting activity towards CDK2. Thus, these results indicate that the phosphorylation status of Thr170 can modulate the substrate specificity of CDK7 to favour CTD over CDKs. Considering the fact that active RNA polymerase II is required for transcription of the viral genome, the inactivation of CAK after administration of ROSC contributes to the downregulation of E6 protein. The restoration of the functional p53 seems to facilitate the induction and execution of apoptosis.

Apart from the anti-viral action of ROSC, the effect of OLO on normal, non-transformed cells is surprising. It increases the cellular levels of the CLIMP-63, alternatively also termed cytoskeleton-associated protein 4/p63 (CKAP4/p63) [31]. OLO induced CLIMP-63 protein in normal, quiescent fibroblasts but not in immortalized or transformed cells [20].

In this context it is worth to mention that CLIMP-63 protein, a non-glycosylated type II integral endoplasmic reticulum (ER) membrane component [47], is a phosphoprotein [48]. The human CLIMP-63 protein, originally identified and cloned by Schweizer and her colleagues [31] consists of 602 amino acids.

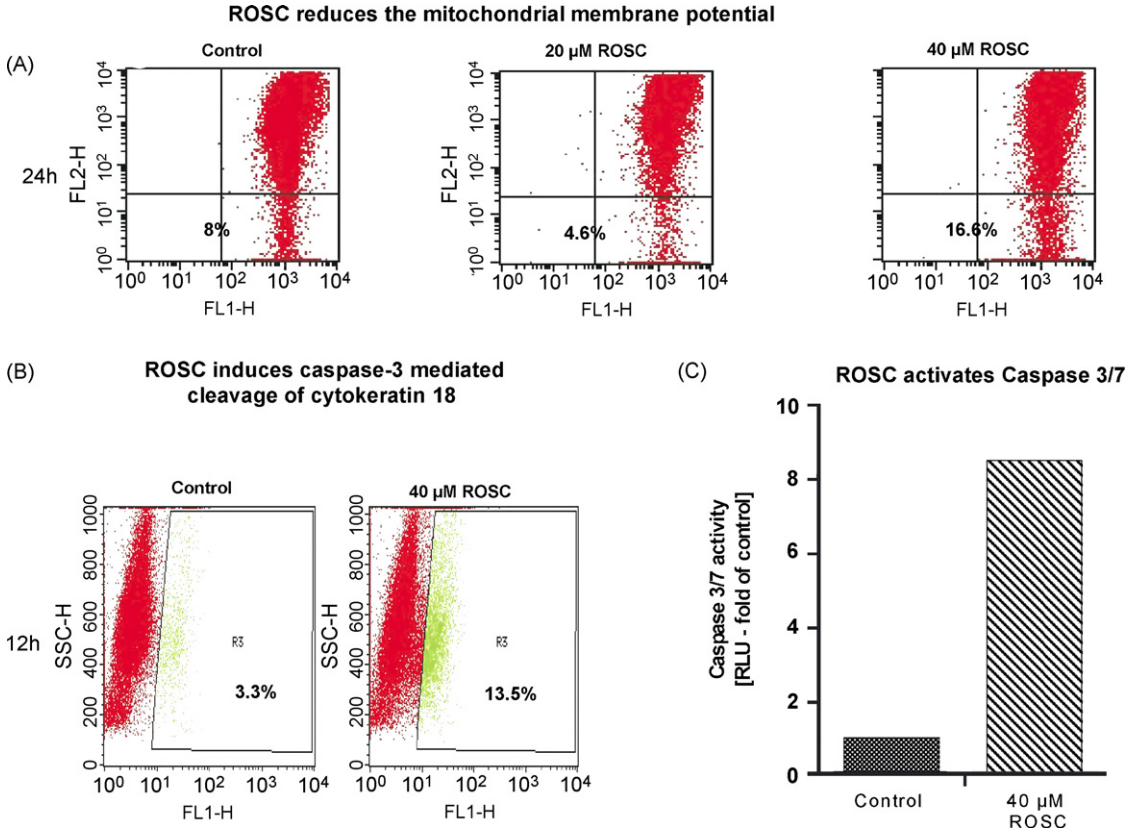

Fig. 8 – ROSC induces caspase-dependent apoptosis. Exponentially growing HeLa cells were exposed to ROSC as indicated. The potential of the mitochondrial membrane (A), caspase-3-mediated cleavage of cytokeratin 18 (B), and activity of caspase-3 (C) were independently determined. (A) Decrease of the mitochondrial membrane potential after exposure to ROSC. Cytogram of green (FL1-H) and red (FL2-H) staining from untreated control and ROSC-treated HeLa cell samples. JC-1 labels mitochondria with high membrane potential (J-aggregates) red and mitochondria with low membrane potential green (JC-1 monomers). The changes in the ratio of green stained cells appearing in the lower right quadrant are indicated. (B) Generation of caspase-3 cleaved cytokeratin 18 during treatment of HeLa cells with ROSC. Cytograms of M30 CytoDEATH-stained cells are shown. (C) Activation of caspase-3/7 in HeLa cells upon treatment with ROSC. Twenty-four hours after plating of HeLa cells into a multiwell plate, medium alone or with ROSC was added. After exposure for 18 h, the numbers of living cells and the activity of caspase-3/7 were determined. Fresh medium (no cells = no caspase) was used as a blank. The measured values (relative luminescence units [RLU]) were blank subtracted and normalized against the number of viable cells present in the wells. Each point represents the average of four replicates. (For interpretation of the references to colour in this figure legend, the reader is referred to the web version of the article).

It contains three main domains: a short NH_2-terminal cytoplasmic segment, a single transmembrane domain, and a large extra-cytoplasmic luminal fragment [31,49]. The cytoplasmic segment binds to microtubules (MTs) [47]. CLIMP-63 protein was first localized to the rough ER of fibroblast-like, epithelial and plasma cells [47]. A few years later it has been reported that CLIMP-63 is also anchored to the cell membrane and may serve as a functional receptor for tissue plasminogen activator [50] and for the frizzled-8 protein-related antiproliferative factor (AIF) [51].

Interestingly, it has been reported that phosphorylation status of CLIMP-63 protein is regulated in a cell cycle-dependent manner and that the extent of its phosphorylation increases during mitosis [48,52]. The cytosolic segment of CLIMP-63 protein contains four typical motifs for phosphorylation, three of which (Ser3, Ser19, and Ser101) are characteristic protein kinase C sites, and one (Ser17) is a casein kinase II site. Phosphorylation of CLIMP-63 protein seems to control CLIMP-63-mediated anchoring of the ER to microtubules [48]. In the light of these observations one might speculate that OLO could reduce the phosphorylation state of CLIMP-63 protein or of microtubules and thereby contribute to its redistribution [48,53]. It could be a result of a changed balance between kinase and phosphatase activities. Since CLIMP-63 protein during interphase links ER membranes to MTs, it is conceivable that changes of the phosphorylation status of MTs could affect their binding to CLIMP-63. Given the possibility that OLO affects the activity of a distinct kinase or phosphatase that directly or indirectly regulates the phosphorylation status of CLIMP-63 protein or MTs, this effect seems to be specific for OLO, because ROSC did not change expression of CLIMP-63 protein. However, this does not explain how the prevention of the phosphorylation of CLIMP-63 protein might affects its stability. One may speculate

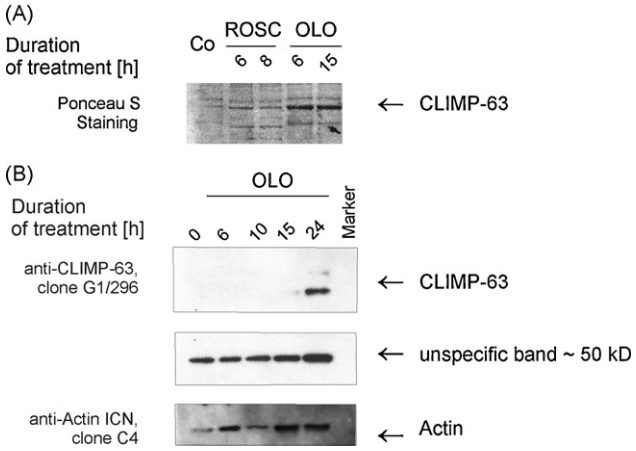

Fig. 9 – OLO induces CLIMP-63 protein in human MRC-5 cells. (A) Induction of a 65 kD protein in OLO-treated MRC-5 cells. Whole cell lysates (WCLs) were prepared from control cells and cells exposed to 20 μM ROSC or to 20 μM OLO for indicated periods of time. Proteins (30 μg protein/well) were resolved on 10% SDS polyacrylamide gels. Proteins were Coomassie-blue stained or transferred onto PVDF membrane and Ponceau stained. (B) Increase of CLIMP-63 protein after exposure to OLO. Blots were incubated with primary antibodies as indicated. Conditions of immunoblotting as described in detail in Fig. 5.

that site-specific phosphorylation could determine the half-life of CLIMP-63 protein as in the case of survivin [54]. It is also conceivable that prevention of phosphorylation would affect the functional organization of CLIMP-63 protein and in this way increase the efficiency of protein synthesis [55].

The functional consequences of the OLO-mediated up-regulation of CLIMP-63 protein in normal, healthy cells and their potential exploitation for, e.g., protection of normal cells from the undesired side effects of chemotherapy have to be systematically elucidated.

Acknowledgments

The authors thank Dr. I. Herbacek for performing flow cytometric measurements and Andreea Borza for performing Western blots. This work was supported at part by a grant P-19894-B11 from the FWF.

REFERENCES

[1] Norbury C, Nurse P. Animal cell cycles and their control. Annu Rev Biochem 1992;61:441–70.
[2] van den Heuvel S, Harlow E. Distinct roles for cyclin-dependent kinases in cell cycle control. Science 1993;262:2050–4.
[3] Morgan DO. Principles of CDK regulation. Nature 1995;374:131–4.
[4] Weinberg RA. The molecular basis of carcinogenesis: understanding the cell cycle clock. Cytokines Mol Ther 1996;2:105–10.
[5] Santamaria D, Ortega S. Cyclins and CDKs in development of cancer. Lessons from genetically modified mice. Front Biosci 2006;11:1164–88.
[6] Malumbres M, Barbacid M. Cell cycle kinases in cancer. Curr Opin Genet Dev 2007;17:60–5.
[7] Senderowicz AM. Small-molecule cyclin-dependent kinase modulators. Oncogene 2003;22:6609–20.
[8] Sherr CJ, Roberts JM. CDK inhibitors: positive and negative regulators of G1-phase progression. Genes Dev 1999;13:1501–12.
[9] de Carcer G, de Castro IP, Malumbres M. Targeting cell cycle kinases for cancer therapy. Curr Med Chem 2007;14:969–85.
[10] Lane DP, Fischer PM. Turning the key on p53. Nature 2004;427:789–90.
[11] Wesierska-Gadek J, Schloffer D, Kotala V, Horky M. Escape of p53 protein from E6-mediated degradation in HeLa cells after cisplatin therapy. Int J Cancer 2002;101:128–36.
[12] Vesely J, Havlicek L, Strnad M, Blow JJ, Donella-Deana A, Pinna L, et al. Inhibition of cyclin-dependent kinases by purine analogues. Eur J Biochem 1994;224:771–86.
[13] Meijer L, Borgne A, Mulner O, Chong JP, Blow JJ, Inagaki N, et al. Biochemical and cellular effects of roscovitine, a potent and selective inhibitor of the cyclin-dependent kinases cdc2, cdk2 and cdk5. Eur J Biochem 1997;243:527–36.
[14] De Azevedo WF, Leclerc S, Meijer L, Havlicek L, Strnad M, Kim SH. Inhibition of cyclin dependent kinases by purine analogues: crystal structure of human cdk2 complexed with roscovitine. Eur J Biochem 1997;243:518–26.
[15] Gray N, Detivaud L, Doerig C, Meijer L. ATP-site directed inhibitors of cyclin-dependent kinases. Curr Med Chem 1999;6:859–75.
[16] Knockaert M, Greengard P, Meijer L. Pharmacological inhibitors of cyclin-dependent kinases. Trends Pharm Sci 2002;23:417–25.
[17] Fischer PM, Gianella-Borradori A. Recent progress in the discovery and development of cyclin-dependent kinase inhibitors. Expert Opin Investig Drugs 2005;14:457–77.
[18] Blagosklonny MV, Demidenko ZN, Fojo T. Inhibition of transcription results in accumulation of Wt p53 followed by delayed outburst of p53-inducible proteins: p53 as a sensor of transcriptional integrity. Cell Cycle 2002;1:67–74.
[19] Wesierska-Gadek J, Schmid G. Dual action of the inhibitors of cyclin-dependent kinases: targeting of the cell cycle progression and activation of wild-type p53 protein. Expert Opin Investig Drugs 2005;14:457–77.
[20] Wesierska-Gadek J, Gueorguieva M, Kramer MP, Ranftler C, Sarg B, Lindner H. A new, unexpected action of olomoucine, a CDK inhibitor, on normal human cells: up-regulation of CLIMP-63, a cytoskeleton-linking membrane protein. J Cell Biochem 2007;102:1405–19.
[21] Wojciechowski J, Horky M, Gueorguieva M, Wesierska-Gadek J. Rapid onset of nucleolar disintegration preceding cell cycle arrest in roscovitine-induced apoptosis of human MCF-7 breast cancer cells. Int J Cancer 2003;106:486–95.
[22] Ljungman M, Paulsen MT. The cyclin-dependent kinase inhibitor roscovitine inhibits RNA synthesis and triggers nuclear accumulation of p53 that is unmodified at Ser15 and Lys382. Mol Pharmacol 2001;60:785–9.
[23] Janicke RU, Sprengart ML, Wati MR, Porter AG. Caspase-3 is required for DNA fragmentation and morphological changes associated with apoptosis. J Biol Chem 1998;273:9357–60.
[24] Devarajan E, Sahin AA, Chen JS, Krishnamurthy RR, Aggarwal N, Brun AM, et al. Down-regulation of caspase 3

in breast cancer: a possible mechanism for chemoresistance. Oncogene 2002;21:8843–51.
[25] Wesierska-Gadek J, Gueorguieva M, Horky M. Dual action of cyclin-dependent kinase inhibitors: induction of cell cycle arrest and apoptosis. A comparison of the effects exerted by roscovitine and cisplatin. Pol J Pharm 2003;55:895–902.
[26] Wesierska-Gadek J, Gueorguieva M, Horky M. Roscovitine-induced up-regulation of p53AIP1 protein precedes the onset of apoptosis in human MCF-7 breast cancer cells. Mol Cancer Ther 2005;4:113–24.
[27] Oda K, Arakawa H, Tanaka T, Matsuda K, Tanikawa C, Mori T, et al. p53AIP1, a potential mediator of p53-dependent apoptosis, and its regulation by Ser-46-phosphorylated p53. Cell 2000;102:849–62.
[28] Wesierska-Gadek J, Schmitz ML, Ranftler C. Roscovitine-activated HIP2 kinase induces phosphorylation of wt p53 at Ser-46 in human MCF-7 breast cancer cells. J Cell Biochem 2007;100:865–74.
[29] Schang LM, Coccaro E, Lacasse JJ. Cdk inhibitory nucleoside analogs prevent transcription from viral genomes. Nucleosides Nucleotides Nucleic Acids 2005;24:829–37.
[30] Schang LM. Discovery of the antiviral activities of pharmacologic cyclin-dependent kinase inhibitors: from basic to applied science. Expert Rev Anti-infective Ther 2005;3:145–9.
[31] Schweizer A, Ericsson M, Bachi T, Griffiths G, Hauri HP. Characterization of a novel 63 kDa membrane protein. Implications for the organization of the ER-to-Golgi pathway. J Cell Sci 1993;104:671–83.
[32] Wesierska-Gadek J, Schloffer D, Gueorguieva M, Uhl M, Skladanowski A. Increased susceptibility of poly(ADP-ribose) polymerase-1 knockout cells to antitumor triazoloacridone C-1305 is associated with permanent G_2 cell cycle arrest. Cancer Res 2004;64:4487–97.
[33] Wesierska-Gadek J, Gueorguieva M, Wojciechowski-Trajkovska S. In vivo activated caspase-3 cleaves PARP-1 in rat liver after administration of the hepatocarcinogen *N*-nitrosomorpholine (NNM) generating the 85 kDa fragment. J Cell Biochem 2004;93(4):774–87.
[34] Wesierska-Gadek J, Gueorguieva M, Ranftler C, Zerza-Schnitzhofer G. A new multiplex assay allowing simultaneous detection of the inhibition of cell proliferation and induction of cell death. J Cell Biochem 2005;96(1):1–7.
[35] Wesierska-Gadek J, Schmid G. Overexpressed poly(ADP-ribose) polymerase delays the release of rat cells from p53-mediated G_1 checkpoint. J Cell Biochem 2000;80:85–103.
[36] Vindelov LL, Christensen IJ, Nissen NJ. A detergent-trypsin method for the preparation of nuclei for flow cytometric DNA analysis. Cytometry 1983;3:323–7.
[37] Wesierska-Gadek J, Wandl S, Kramer MP, Pickem C, Krystof V, Hajek SB. Roscovitine up-regulates p53 protein and induces apoptosis in human HeLaS3 cervix carcinoma cells. J Cell Biochem 2008 DOI 10.1002/jcb.21903.
[38] Murray AW, Marks D. Can sequencing shed light on cell cycling? Nature 2001;409:844–6.
[39] Fisher RP. Secrets of a double agent: CDK7 in cell-cycle control and transcription. J Cell Sci 2005;118:5171–80.
[40] Palancade B, Bensaude O. Investigating RNA polymerase II carboxyl-terminal domain (CTD) phosphorylation. Eur J Biochem 2003;270:3859–70.
[41] Meinhart A, Kamenski T, Hoeppner S, Baumli S, Cramer P. A structural perspective of CTD function. Genes Dev 2005;19:1401–15.
[42] Marshall RM, Grana X. Mechanisms controlling CDK9 activity. Front Biosci 2006;11:2598–613.
[43] Scheffner M, Huibregtse JM, Vierstra RD, Howley PM. The HPV-16 E6 and E6-AP complex functions as a ubiquitin-protein ligase in the ubiquitination of p53. Cell 1993;75:495–505.
[44] Scheffner M, Werness BA, Huibregtse JM, Levine AJ, Howley PM. The E6 oncoprotein encoded by human papillomavirus types 16 and 18 promotes the degradation of p53. Cell 1990;63:1129–36.
[45] Goodwin EC, DiMaio D. Repression of human papillomavirus oncogenes in HeLa cervical carcinoma cells causes the orderly reactivation of dormant tumor suppressor pathways. Proc Natl Acad Sci 2000;97:12513–8.
[46] Wang W, Deiry WS El. Restoration of p53 to limit tumor growth. Curr Opin Oncol 2008;20:90–6.
[47] Schweizer A, Rohrer J, Slot JW, Geuze HJ, Kornfeld S. Reassessment of the subcellular localization of p63. J Cell Sci 1995;108(Pt 6):2477–85.
[48] Vedrenne C, Klopfenstein DR, Hauri HP. Phosphorylation controls CLIMP-63-mediated anchoring of the endoplasmic reticulum to microtubules. Mol Biol Cell 2005;16(4):1928–37.
[49] Klopfenstein DR, Klumperman J, Lustig A, Kammerer RA, Oorschot V, Hauri HP. Subdomain-specific localization of CLIMP-63 (p63) in the endoplasmic reticulum is mediated by its luminal alpha-helical segment. J Cell Biol 2001;153(6):1287–300.
[50] Razzaq TM, Bass R, Vines DJ, Werner F, Whawell SA, Ellis V. Functional regulation of tissue plasminogen activator on the surface of vascular smooth muscle cells by the type-II transmembrane protein p63 (CKAP4). J Biol Chem 2003;278(43):42679–85.
[51] Conrads TP, Tocci GM, Hood BL, Zhang CO, Guo L, Koch KR, et al. CKAP4/p63 is a receptor for the frizzled-8 protein-related antiproliferative factor from interstitial cystitis patients. J Biol Chem 2006;281:37836–43.
[52] Pignolo RJ, Rotenberg MO, Horton JH, Cristofalo VJ. Senescent WI-38 fibroblasts overexpress LPC-1, a putative transmembrane shock protein. Exp Cell Res 1998;240(2):305–11.
[53] Nikonov AV, Hauri HP, Lauring B, Kreibich G. Climp-63-mediated binding of microtubules to the ER affects the lateral mobility of translocon complexes. J Cell Sci 2007;120(Pt 13):2248–58.
[54] Wall NR, O'Connor DS, Plescia J, Pommier Y, Altieri DC. Suppression of survivin phosphorylation on Thr34 by flavopiridol enhances tumor cell apoptosis. Cancer Res 2003;63(1):230–5.
[55] Nikonov AV, Kreibich G. Organization of translocon complexes in ER. Biochem Soc Trans 2003;31(Pt 6):1253–6.